Prediction of Jump Phenomena in Aircraft Maneuvers, including Nonlinear Aerodynamic Effects

J. W. Young,* A.A. Schy,† and K.G. Johnson*
NASA Langley Research Center, Hampton, Va.

An analytical method has been developed for predicting critical control inputs for which nonlinear rotational coupling may cause sudden jumps in aircraft response. The analysis includes the effects of aerodynamics, which are nonlinear in angle of attack. The method involves the simultaneous solution of two polynomials in roll rate, whose coefficients are functions of angle of attack and the control inputs. Results obtained using this procedure are compared with calculated time histories to verify the validity of the method for predicting jumplike instabilities.

Introduction

MANEUVERING airplanes sometimes undergo sudden divergent motions not predicted by the usual linearized response analysis. Since the study of Phillips,[1] which predicted a "roll coupling" divergence for a range of roll rates, many extensions of his analysis have been published. Pinsker[2] and Rhoads and Schuler[3] showed that Phillips' critical roll rates were related to pseudosteady solutions of the equations of motion. They also conjectured that the "jump" phenomena observed in simulated maneuver calculations were transitions from one pseudosteady solution to another. Generally, however, analyses of this problem have aimed primarily at obtaining predictions of peak incidence angles (α and β) in maneuvers, using roll rate as the independent parameter. A recent paper by Hacker and Oprisiu[4] makes an important contribution in this direction by accounting for gravity effects, using g/V as a small parameter in a series expansion. They also present a review of previous work and an excellent bibliography.

The present study is based on the belief that accurate analytical prediction of peak values in coupled maneuvers is not as important as reliable prediction of critical conditions for which jump phenomena may occur, since accurate dynamic simulations are generally available which can calculate the motions in the critical conditions when these have been identified. Therefore, in this analysis, the control deflections are made the independent variables, and an analytical method is developed for predicting critical control inputs for which nonlinear rotational coupling may cause sudden jumps in aircraft response. A previous paper[5] described a simplified version of the method in which aerodynamic effects were assumed to be linear. The objective of the current study is to extend the analysis of Ref. 5 to permit the aerodynamic effects to be arbitrary functions of angle of attack.

In Ref. 5, pseudosteady-state solutions were obtained by solving a single polynomial in roll rate with coefficients that were functions of the control inputs. The present analysis requires the simultaneous solution of two polynomials in roll rate whose coefficients are functions of angle of attack and the control inputs. As in Ref. 5, the solutions are referred to as pseudosteady states (PSS), since they neglect the effect of varying weight components in the body axis.

Results obtained using the PSS prediction procedure will be given for a variety of maneuvers by a fighter-type aircraft. Time history responses also will be presented to validate the prediction procedure.

Received June 22, 1977; presented as Paper 77-1126 at the AIAA 4th Atmospheric Flight Mechanics Conference, Hollywood, Fla., Aug. 8-10, 1977 (in bound volume of Conference papers); revision received Sept. 1, 1977.

Index category: Handling Qualities, Stability and Control.

*Aerospace Engineer.
†Supervisory Aerospace Engineer. Associate Fellow AIAA.

Analysis

The nonlinear equations of motion used in the calculation of all time history responses are given in the Appendix. Air density and speed are assumed to be constant, and sideslip angle (β) is assumed to be small. Principal axes are used.

To obtain equilibrium or steady-state solutions, it is necessary to solve the nonlinear equations of the Appendix with all time derivatives set to zero. This approach was used in Ref. 6 to calculate equilibrium spin conditions for aircraft. Because of the vertical weight force, the resulting motions of Ref. 6 consisted of spiral paths about a vertical axis. The pseudosteady states differ from these true steady states in that the Euler angle variations, which determine the weight component variations in body axes, are ignored. This approximation is appropriate in analyzing rotational coupling effects in rapid maneuvers, since it eliminates the constraint that the rotational velocity be about the vertical axis. This was achieved by ignoring the $\dot{\phi}$ and $\dot{\theta}$ equations in the PSS analysis and assuming $\theta=\theta_0$ and $\phi=0$ in the g/V terms in the force equations (i.e., the $\dot{\alpha}$ and $\dot{\beta}$ equations) of the Appendix. The resulting five equations, with their time derivatives set to zero, are used in the following analysis to obtain PSS solutions.

Solution for Pseudosteady States

The equations used in the PSS analysis can be written as

$$\bar{p}\bar{q}-\bar{\beta}\hat{n}_\beta(\bar{\alpha})-\bar{r}\hat{n}_r(\bar{\alpha})=\hat{n}_0(\bar{\alpha},\delta_a,\delta_r)+\bar{p}\hat{n}_p(\bar{\alpha}) \quad (1)$$

$$\bar{q}\hat{m}_q(\bar{\alpha})+\bar{p}\bar{r}=-\hat{m}_0(\bar{\alpha},\delta_e) \quad (2)$$

$$-\bar{q}+\bar{p}\bar{\beta}=Z_0(\bar{\alpha},\delta_e) \quad (3)$$

$$-\bar{r}\cos\bar{\alpha}+\bar{p}\sin\bar{\alpha}+\bar{\beta}y_\beta(\bar{\alpha})+\bar{p}y_p(\bar{\alpha})+\bar{r}y_r(\bar{\alpha})+y_0(\bar{\alpha},\delta_a,\delta_r)=0 \quad (4)$$

$$\beta\hat{l}_\beta/(\bar{\alpha})+r\hat{l}_r(\bar{\alpha})+\bar{p}\hat{l}_p(\bar{\alpha})+\hat{l}_0(\bar{\alpha},\delta_a,\delta_r)=\bar{q}\bar{r} \quad (5)$$

where

$$\hat{n}_0(\bar{\alpha},\delta_a,\delta_r)=\hat{n}_{\delta_a}(\bar{\alpha})\delta_a+\hat{n}_{\delta_r}(\bar{\alpha})\delta_r$$

$$\hat{m}_0(\bar{\alpha},\delta_e)=\hat{m}(\bar{\alpha})+\hat{m}_{\delta_e}(\bar{\alpha})\delta_e$$

$$Z_0(\bar{\alpha}, \delta_e) = Z(\bar{\alpha}) + Z_{\delta_e}(\bar{\alpha})\delta_e + (g/V)\cos\theta_0$$

$$y_0(\bar{\alpha}, \delta_a, \delta_r) = y_{\delta_a}(\bar{\alpha})\delta_a + y_{\delta_r}(\bar{\alpha})\delta_r$$

$$\hat{l}_0(\bar{\alpha}, \delta_a, \delta_r) = \hat{l}_{\delta_a}(\bar{\alpha})\delta_a + \hat{l}_{\delta_r}(\bar{\alpha})\delta_r$$

The overbars in the preceding equations indicate PSS solutions. Hereafter, for convenience, the arguments for the aerodynamic coefficients will be dropped.

Equations (1-3) are linear in $\bar{q}$, $\bar{\beta}$, $\bar{r}$ and can be solved for these variables as functions of $\bar{p}$, $\bar{\alpha}$, and the control inputs. These equations can be written in matrix form as follows:

$$\begin{bmatrix} \bar{p} & -\hat{n}_r & \hat{n}_\beta \\ \hat{m}_q & \bar{p} & 0 \\ -1 & 0 & \bar{p} \end{bmatrix} \begin{bmatrix} \bar{q} \\ \bar{r} \\ \bar{\beta} \end{bmatrix} = \begin{bmatrix} \hat{n}_0 \\ -\hat{m}_0 \\ Z_0 \end{bmatrix} + \bar{p} \begin{bmatrix} \hat{n}_p \\ 0 \\ 0 \end{bmatrix} \quad (6a)$$

The determinant of the preceding matrix is given by

$$D(\bar{\alpha}, \bar{p}) = \bar{p}^3 - \bar{p}(\hat{n}_\beta - \hat{m}_q\hat{n}_r) \quad (6b)$$

Solutions for q, r, and β are as follows:

$$\bar{q} = [\,\hat{n}_p\bar{p}^3 + \hat{n}_0\bar{p}^2 + \bar{p}(\hat{n}_\beta Z_0 - \hat{m}_0\hat{n}_r)\,]/D \quad (7)$$

$$\bar{r} = [\,-\bar{p}^2(\hat{m}_0 + \hat{m}_q\hat{n}_p) - \bar{p}\hat{m}_q\hat{n}_0 + \hat{n}_\beta(\hat{m}_0 - Z_0\hat{m}_q)\,]/D \quad (8)$$

$$\bar{\beta} = [\bar{p}^2(Z_0 + \hat{n}_p) + \bar{p}\hat{n}_0 - \hat{n}_r(\hat{m}_0 - Z_0\hat{m}_q)\,]/D \quad (9)$$

Substituting these values for $\bar{q}$, $\bar{r}$, and $\bar{\beta}$ into Eq. (4) gives the following quartic in $\bar{p}$:

$$A_4\bar{p}^4 + A_3\bar{p}^3 + A_2\bar{p}^2 + A_1\bar{p} + A_0 = 0 \quad (10)$$

where

$$A_4 = y_p + \sin\bar{\alpha}$$

$$A_3 = y_0$$

$$A_2 = y_\beta(Z_0 + \hat{n}_p) + (y_p + \sin\bar{\alpha})(\hat{m}_q\hat{n}_r - \hat{n}_\beta) - (y_r - \cos\bar{\alpha})(\hat{m}_0 + \hat{m}_q\hat{n}_p)$$

$$A_1 = y_0(\hat{m}_q\hat{n}_r - \hat{n}_\beta) + \hat{n}_0[y_\beta - \hat{m}_q(y_r - \cos\bar{\alpha})]$$

$$A_0 = -(\hat{m}_0 - Z_0\hat{m}_q)[y_\beta\hat{n}_r - \hat{n}_\beta(y_r - \cos\bar{\alpha})]$$

The final equation to be considered is the rolling Eq. (5). In most roll-coupling studies, the qr product is assumed to be of minor influence and is neglected. Here, both cases $qr = 0$ and $qr \neq 0$ are presented. Substituting Eqs. (7-9) into Eq. (5) with $qr = 0$ yields the following quartic in $\bar{p}$:

$$B_4\bar{p}^4 + B_3\bar{p}^3 + B_2\bar{p}^2 + B_1\bar{p} + B_0 = 0 \quad (11)$$

where

$$B_4 = \hat{l}_p$$

$$B_3 = \hat{l}_0$$

$$B_2 = \hat{l}_p(\hat{m}_q\hat{n}_r - \hat{n}_\beta) + \hat{l}_\beta(Z_0 + \hat{n}_p) - \hat{l}_r(\hat{m}_0 + \hat{m}_q\hat{n}_p)$$

$$B_1 = \hat{l}_0(\hat{m}_q\hat{n}_r - \hat{n}_\beta) + \hat{n}_0(\hat{l}_\beta - \hat{l}_r\hat{m}_q)$$

$$B_0 = (\hat{m}_0 - Z_0\hat{m}_q)(\hat{l}_r\hat{n}_\beta - \hat{l}_\beta\hat{n}_r)$$

For the case where the qr term is included, we obtain from Eq. (5)

$$C_6\bar{p}^6 + C_5\bar{p}^5 + C_4\bar{p}^4 + C_3\bar{p}^3 + C_2\bar{p}^2 + C_1\bar{p} + C_0 = 0 \quad (12)$$

where

$$C_6 = \hat{l}_p$$

$$C_5 = \hat{l}_0$$

$$C_4 = (\hat{m}_0 + \hat{m}_q\hat{n}_p)(\hat{n}_p - \hat{l}_r) + 2\hat{l}_p(\hat{m}_q\hat{n}_r - \hat{n}_\beta) + \hat{l}_\beta(Z_0 + \hat{n}_p)$$

$$C_3 = \hat{n}_0[\hat{m}_0 + \hat{l}_\beta + \hat{m}_q(2\hat{n}_p - \hat{l}_r)\,] + 2\hat{l}_0(\hat{m}_q\hat{n}_r - \hat{n}_\beta)$$

$$C_2 = (\hat{m}_0 - Z_0\hat{m}_q)(\hat{l}_r\hat{n}_\beta - \hat{l}_\beta\hat{n}_r - \hat{n}_\beta\hat{n}_p) + (\hat{n}_\beta Z_0 - \hat{m}_0\hat{n}_r)(\hat{m}_0 + \hat{m}_q\hat{n}_p) + (\hat{m}_q\hat{n}_r - \hat{n}_\beta)[\hat{l}_p(\hat{m}_q\hat{n}_r - \hat{n}_\beta) + \hat{l}_\beta(Z_0 + \hat{n}_p) - \hat{l}_r(\hat{m}_0 + \hat{m}_q\hat{n}_p)\,] + \hat{n}_0{}^2\hat{m}_q$$

$$C_1 = (\hat{m}_q\hat{n}_r - \hat{n}_\beta)[\hat{l}_0(\hat{m}_q\hat{n}_r - \hat{n}_\beta) + \hat{n}_0(\hat{l}_\beta - \hat{l}_r\hat{m}_q)\,] - \hat{n}_0\hat{n}_\beta(\hat{m}_0 - Z_0\hat{m}_q) + \hat{n}_0\hat{m}_q(\hat{n}_\beta Z_0 - \hat{m}_0\hat{n}_r)$$

$$C_0 = (\hat{m}_0 - Z_0\hat{m}_q)[(\hat{m}_q\hat{n}_r - \hat{n}_\beta)(\hat{l}_r\hat{n}_\beta - \hat{l}_\beta\hat{n}_r) - \hat{n}_\beta(\hat{n}_\beta Z_0 - \hat{m}_0\hat{n}_r)\,]$$

Consider the case where $qr = 0$. Simultaneous solutions of Eqs. (10) and (11) will yield PSS values for $\bar{p}$ and $\bar{\alpha}$ for specified values of the control inputs. Various iterative search algorithms could be used to find values for $\bar{p}$ and $\bar{\alpha}$ which satisfy Eqs. (10) and (11). The search procedure employed in the present study will be described now.

For fixed values of the control inputs, a "sweep" is made through the angle-of-attack range under consideration. Solutions to Eq. (10) are obtained at each of these $\bar{\alpha}$ values. The $\bar{p}$ solutions, if real, are substituted into Eq. (11), and residuals are computed for each value of $\bar{p}$. If the residuals from Eq. (11) change sign between successive values for $\bar{\alpha}$, a common root of Eqs. (10) and (11) exists. If the common root is not a root of the determinant [Eq. (6b)], an iterative procedure calculates the angle of attack required to reduce the residual to within a specified tolerance. Having determined the $\bar{p}$ and $\bar{\alpha}$ values that satisfy Eqs. (10) and (11), $\bar{q}$, $\bar{r}$, and $\bar{\beta}$ are computed from Eqs. (7-9). The linearized stability characteristics for perturbations about the PSS solution then are calculated. The $\bar{\alpha}$ sweep is continued until all PSS solutions are obtained for the specified set of control inputs.

For the case where $qr \neq 0$, the search procedure is the same, with residuals being computed from Eq. (12) instead of Eq. (11). This search procedure has been implemented on both a high-speed and a minicomputer, and solutions to the two polynomials can be attained rapidly for any combination of elevator, aileron, and rudder.

Stability of PSS Solutions

The stability of the PSS solution was calculated by inserting the PSS solutions into the first five equations of the Appendix and linearizing about the PSS values. The matrix whose characteristic roots determine the stability of the perturbed motion is

$$A = \begin{bmatrix} n_r & -J_z\bar{p} & n' & n_\beta & n_p - J_z\bar{q} \\ J_y\bar{p} & \bar{m}_q & m' & 0 & J_y\bar{r} \\ 0 & 1 & Z' & -\bar{p} & -\bar{\beta} \\ y_r - \cos\bar{\alpha} & 0 & \bar{p} + Y' & y_\beta & y_p + \sin\bar{\alpha} \\ l_r - J_x\bar{q} & -J_x\bar{r} & l' & l_\beta & l_p \end{bmatrix}$$

$$J_x = \frac{I_Z - I_Y}{I_X}, \quad J_y = \frac{I_Z - I_X}{I_Y}, \quad J_z = \frac{I_Y - I_X}{I_Z}$$

Also,

$$Y' = y_{\beta_\alpha}\bar{\beta} + y_{p_\alpha}\bar{p} + y_{r_\alpha}\bar{r} + y_{\delta a_\alpha}\delta_a + y_{\delta r_\alpha}\delta_r$$

$$Z' = Z_\alpha + Z_{\delta e_\alpha}\delta_e$$

$$l' = l_{\beta_\alpha}\bar{\beta} + l_{p_\alpha}\bar{p} + l_{r_\alpha}\bar{r} + l_{\delta a_\alpha}\delta_a + l_{\delta r_\alpha}\delta_r$$

$$m' = m_\alpha + m_{\delta e_\alpha}\delta_e$$

$$n' = n_{\beta_\alpha}\bar{\beta} + n_{p_\alpha}\bar{p} + n_{r_\alpha}\bar{r} + n_{\delta a_\alpha}\delta_a + n_{\delta r_\alpha}\delta_r$$

The absence of carets on the moment derivatives indicates that the inertia ratios are not factored out as in the equations of the Appendix. For example, $n_\beta = \bar{q}SbC_{n_\beta}/I_Z$.

It should be noted that the stability characteristics as defined by Eqs. (13) are approximate, since the effects of the varying weight components are neglected. Also, stability derivatives in column 3 of [A] were obtained by computing numerical slopes. This procedure can introduce discontinuities in these stability derivatives at break points in the tabular aerodynamic data used in the computer program. These approximate stability characteristics were considered adequate for this exploratory study, since the PSS solutions are only approximate steady states.

Aircraft Characteristics

Variations with angle of attack of the significant aerodynamic coefficients used in the analysis are given in Figs. 1 and 2. For $\alpha < 30$ deg, these data were obtained from a simulation of a fighter airplane flying at 45,000 ft and Mach number 0.9 ($V = 870$ ft/s and dynamic pressure $= 175$ lb/ft^2). To extend these data to higher angles of attack in a simple manner, values for each curve were chosen at $\alpha = 35$ and 40 deg, which could be extrapolated linearly to give reasonable values at higher angles of attack. The principal axis inertia characteristics I_X, I_Y, and I_Z for the assumed aircraft are 24,960; 122,186; and 139,800 slug-ft^2, respectively.

Results and Discussion

The method has been applied to a number of examples for the assumed aircraft. Three of these examples will be examined in the present paper. The first of these is for aileron-roll maneuvers that are initiated from a 1-g trim condition ($L = W$, pitching moment $= 0$). In the second case, a pitch-down elevator that produces a negative-g maneuver ($-0.65\ g$) is used in combination with the aileron. In the final example, a pitch-up elevator that corresponds to a 2.1-g pull-up is applied, together with the aileron. PSS solutions will be discussed for each of these three examples. Time history responses then will be presented to validate the PSS analysis.

PSS Solutions

As discussed in Ref. 5, the existence of multiple PSS solutions can lead to predictions of jumps in the response at certain control input combinations in two situations. If the basic solution disappears at some control combination, the response certainly would be expected to jump to the vicinity of another PSS solution. Also, if the basic solution remains stable but comes close to another solution, the perturbed response may enter the domain of influence of this other solution, and a jump may occur. In some examples of Ref. 5, this occurred when the nearby solution has a divergent stability characteristic. The response then jumped (diverged) to the vicinity of another stable solution. In this type of example, the prediction of the jump responses is not as clear as it is when the basic solution disappears. However, the main purpose of the PSS analysis is to predict when jumps may occur, so that these cases may be examined in detail in a complete six-degree-of-freedom simulator program. These two possible types of jump response prediction now will be used in analyzing the PSS solutions for the three example cases.

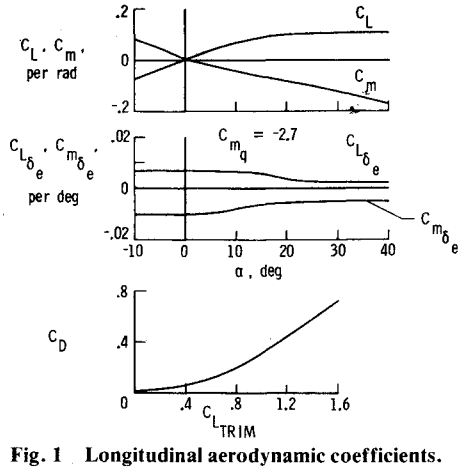

Fig. 1 Longitudinal aerodynamic coefficients.

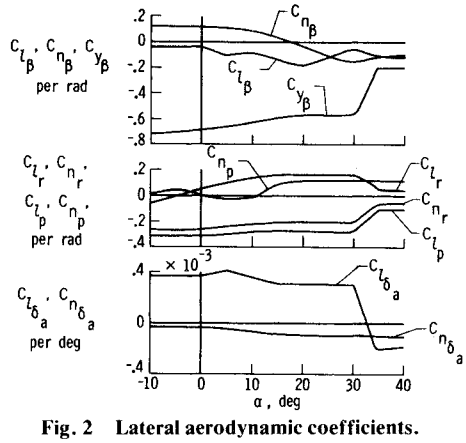

Fig. 2 Lateral aerodynamic coefficients.

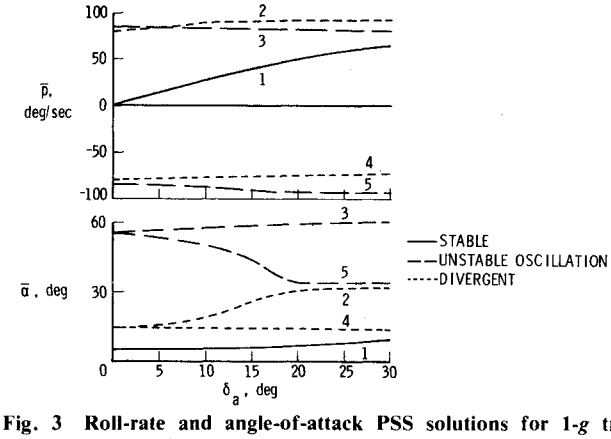

Fig. 3 Roll-rate and angle-of-attack PSS solutions for 1-g trim condition ($\delta_e = -2.8$ deg).

One-g Trim

Figure 3 shows PSS solutions for roll rate and angle of attack at various aileron inputs for the 1-g trim flight condition. Solid lines represent stable solutions. Dotted lines represent conditions from which a divergence would occur. Dashed lines should be considered potential attractors, since they contain only a slightly unstable oscillation. Also, as previously mentioned, the approximate nature of the stability analysis makes it impossible to distinguish between marginally stable or unstable modes.

As shown in Fig. 3, there are five PSS solutions at each aileron input. The basic solution (curve 1, starting at $\bar{p} = 0$ and $\delta_a = 0$ deg) represents the only stable condition. All other PSS solutions are either divergent or oscillatory unstable. Since the

basic solution remains stable for all aileron deflections, the only possibility for a jump prediction is if the basic solution gets close enough to curves 2 or 3 to come within their domain of attraction. Although the basic $\bar{p}$ solutions of Fig. 3 do seem to come close, the $\bar{\alpha}$ solutions are still far apart at $\delta_a = 30$ deg. Since α is such an important parameter in determining the characteristics with nonlinear aerodynamics, it seems very unlikely that a jump would occur. Nevertheless, there is enough uncertainty in this case to require confirmation by checking simulated responses.

The results of Fig. 3, as well as for the remaining PSS solutions to be presented, were calculated under the assumption that the product qr [Eq. (5)] is negligible. A limited number of results were obtained for which the qr term was included. Inclusion of this term was found to increase the computational difficulty of obtaining simultaneous solutions to the two polynomials. However, only minor differences existed between the PSS values obtained, and no new solutions were introduced for the cases considered. Future studies will investigate the significance of the qr contribution.

Negative-g Maneuver

Figure 4 shows PSS solutions for $\bar{p}$, $\bar{\alpha}$, and $\bar{\beta}$ for the $-0.65g$ maneuver. [The $\bar{\beta}$ solutions for curves 5 and 6 are not shown, since they remain small ($|\beta| < 2$ deg) for all aileron deflections.] For aileron levels less than about 15 deg, five PSS solutions exist with only the basic solution (curve 1) being stable. At about $\delta_a = 16$ deg, two additional divergent PSS solutions appear. Also, for aileron levels greater than about 20 deg, the basic solution disappears, and curve 4 becomes stable. Thus, we would expect a jump in roll rate for δ_a greater than about 20 deg. Since curve 4 is the only stable PSS solution at large aileron deflections, we would expect $\bar{p}$ to attain the levels shown on curve 4.

Solution 5 is a very unusual one. It might appear from Fig. 4a that this solution might play an important role in any jump responses for $\delta_a > 20$ deg, since this $\bar{p}$ solution is near the curve 1 values. However, Fig. 4b shows that $\bar{\alpha}_5$ is very far from $\bar{\alpha}_1$, so that (as in the previous case) these two solutions are not really close in state space.

Positive-g Maneuver

Figure 5 shows PSS solutions for the 2.1-g pull-up condition. Note that there is a roll reversal (positive aileron normally gives positive p) in the basic solution (curve 1) and that the solution disappears for ailerons greater than about 4 deg. Also, only divergent and oscillatory unstable PSS solutions exist for $\delta_a > 4$ deg. Since the predicted roll rates for the basic solution are very low, even when it disappears, there is some doubt of the validity of the PSS approximation that varying weight components are of secondary importance. This approximation assumes rapid maneuvers, in which the aerodynamic moments and rotational coupling effects are dominant. Therefore, this case should provide an interesting test of the range of validity of the PSS analysis. The predictions from the results of Fig. 5 would be that there is a roll-rate reversal for very small aileron inputs, that some sort of jump should occur for inputs greater than approximately 4 deg, and that very irregular responses would be expected for larger inputs, since there are no stable solutions.

Time History Responses

Time history responses now will be presented to validate the PSS results of Figs. 3-5. Unless noted, all time histories were calculated with the varying gravity components included.

One-g Trim

Time history calculations were found to be in good agreement with the PSS predictions of Fig. 3. At all aileron deflections, the steady-state value for all variables was close to those predicted by the basic solution (curve 1) on Fig. 3. Calculated roll-rate responses to aileron values of 15 and 30 deg are shown in Fig. 6. As can be seen, the responses are

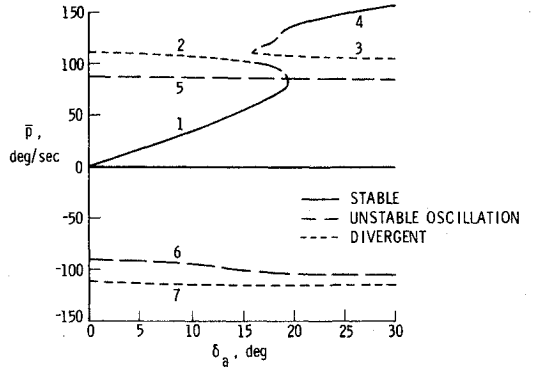

a) Roll rate.

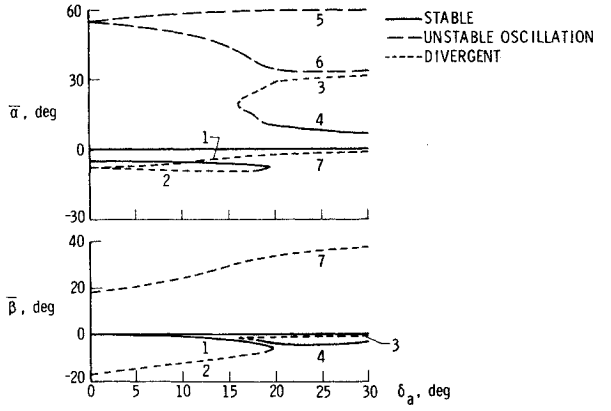

b) Angle of attack and sideslip

Fig. 4 PSS solutions for negative-g maneuver ($\delta_e = 4$ deg).

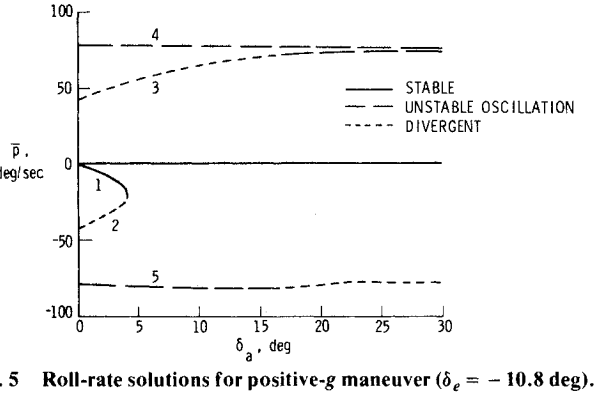

Fig. 5 Roll-rate solutions for positive-g maneuver ($\delta_e = -10.8$ deg).

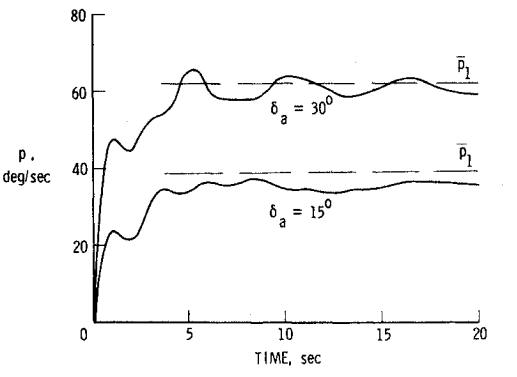

Fig. 6 Calculated roll-rate responses initiated from 1-g trim condition for two aileron inputs ($\delta_e = -2.8$ deg, $\alpha_0 = 5.4$ deg).

close to the PSS prediction. Similar agreement was found for α, q, r, and β.

Negative-g Maneuver

The PSS solution of Fig. 4 predicted a jump in aircraft response for values of aileron greater than about 20 deg for the negative-g maneuver. Time history calculations verified this response, as well as the other PSS predictions of Fig. 4. For $\delta_a < 20$ deg, the steady-state responses were close to those predicted by curve 1 of Fig. 4. The jump occurred for $\delta_a = 20$ deg on time histories calculated with constant gravity. On time histories that included varying gravity components, the jump occurred for aileron deflections of about 22 deg or greater.

Figure 7 illustrates the aircraft response before and after a roll-coupled jump for the negative-g maneuver (varying gravity components included). For this case, the aileron was maintained at 18 deg for the first 5 s and then increased to 24 deg for the remainder of the run. The p, α, and β responses at 5 s are in good agreement with the PSS predictions on the basic curve of Fig. 4 for $\delta_a = 18$ deg. When the aileron is set at 24 deg after 5 s, the tendency to diverge is evident first in β and p. Apparently the increasingly negative sideslip acts through the dihedral effect to accelerate the rolling. Finally, after around 12 s, α suddenly diverges toward the positive PSS solution of curve 4 on Fig. 4, and all of the responses show violent oscillations in the vicinity of this PSS solution.

Although the initial rapid divergence associated with roll-coupling is the important aspect of the analysis, it is of interest to check the PSS predictions following a jump. Continuation of the history of Fig. 7 beyond 20 s would show p, α, and β gradually converging to values near the PSS predictions. This is illustrated better by using aileron levels further removed from the critical aileron region of about 20-22 deg. Shown in Fig. 8 are p, α, and β histories for an aileron of 30 deg. As shown, the postjump responses are close to the PSS predictions of Fig. 4.

Positive-g Maneuver

As previously mentioned, the low roll rates associated with the positive-g maneuver are not of the type for which the roll-coupling analysis was intended. Although precise predictions of critical control inputs would not be expected in this case when the simulated responses include the rotationally varying weight components, it is interesting to examine the time histories as a check of the range of validity of the PSS predictions. Note that the results in Fig. 5 predicted roll reversal at small aileron values, and that there were no stable solutions after the basic solution disappeared at aileron values greater than 4 deg.

Time histories without varying gravity components were in good agreement with the PSS predictions of Fig. 5, with the jump occurring at an aileron of about 4 deg. When varying gravity components were included, the jump was slower in developing and occurred at an aileron of about 6 deg.

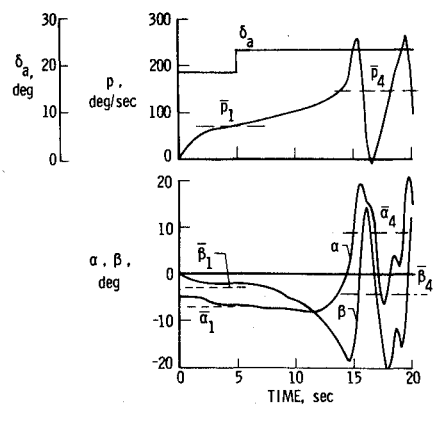

Fig. 7 Calculated responses initiated from negative-g condition ($\delta_e = 4$ deg, $\alpha_0 = -5.1$ deg).

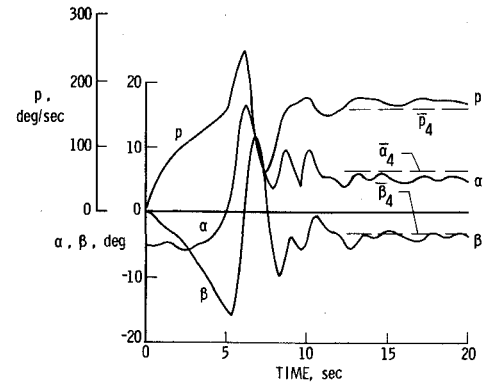

Fig. 8 Calculated responses initiated from negative-g condition for $\delta_a = 30$ deg, $\delta_e = 4$ deg, $\alpha_0 = -5.1$ deg.

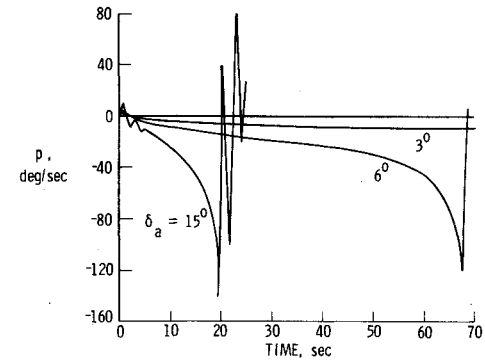

Fig. 9 Calculated roll-rate responses initiated from positive-g condition ($\delta_e = -10.8$ deg, $\alpha_0 = 16.6$ deg).

Shown in Fig. 9 are roll-rate responses at three aileron levels for the constant-gravity case. The roll reversal prediction of Fig. 5 is verified in Fig. 9. For $\delta_a = 3$ deg, the roll-rate response is in agreement with the basic solution (curve 1) of Fig. 5. For $\delta_a = 6$ and 15 deg, the jump is seen to occur. Following the jump, wild oscillations occur in all trajectory variables, since no stable solutions are present.

The results that have been presented are of a preliminary nature and have validated the PSS analysis. In the present analysis, rudder inputs were not included. Future studies will include the combined effects of aileron, elevator, and rudder and will investigate a variety of practical aircraft examples. The importance of the qr contribution also will be investigated for a wider range of examples.

Concluding Remarks

A method has been presented for predicting critical control combinations that may lead to jump phenomena in rotationally coupled maneuvers of aircraft. This pseudosteady-state analysis permits the aerodynamics to be arbitrary functions of angle of attack. The method was applied to several examples for a fighter-type aircraft. Time history responses verified the validity of the procedure for predicting jumplike instabilities.

Appendix

The nonlinear equations of motion used in the calculation of response time histories are as follows:

$$\dot{r} = \frac{I_Y - I_X}{I_Z}\left[-pq + \beta \hat{n}_\beta(\alpha) + p\hat{n}_p(\alpha) + r\hat{n}_r(\alpha) + \hat{n}_{\delta_a}(\alpha)\delta_a + \hat{n}_{\delta_r}(\alpha)\delta_r\right] \quad \text{(A1)}$$

$$\dot{q}=\frac{I_Z-I_X}{I_Y}[pr+q\hat{m}_q(\alpha)+\dot{\alpha}\hat{m}_{\dot{\alpha}}(\alpha)+\hat{m}(\alpha)+\hat{m}_{\delta_e}(\alpha)\delta_e] \quad \text{(A2)}$$

$$\dot{\alpha}=q-p\beta+Z(\alpha)+Z_{\delta_e}(\alpha)\delta_e+(g/V)\cos\theta\cos\phi \quad \text{(A3)}$$

$$\dot{\beta}=-r\cos\alpha+p\sin\alpha+\beta y_\beta(\alpha)+py_p(\alpha)+ry_r(\alpha)+y_{\delta_a}(\alpha)\delta_a+y_{\delta_r}(\alpha)\delta_r+(g/V)\cos\theta\sin\phi \quad \text{(A4)}$$

$$\dot{p}=\frac{I_Z-I_Y}{I_X}[-qr+\beta\hat{l}_\beta(\alpha)+p\hat{l}_p(\alpha)+r\hat{l}_r(\alpha)+\hat{l}_{\delta_a}(\alpha)\delta_a+\hat{l}_{\delta_r}(\alpha)\delta_r] \quad \text{(A5)}$$

$$\dot{\phi}=p+\tan\theta(q\sin\phi+r\cos\phi) \quad \text{(A6)}$$

$$\dot{\theta}=q\cos\phi-r\sin\phi \quad \text{(A7)}$$

The preceding equations are written in principal axes, with the assumption that speed and air density are constant and that $\sin\beta=\beta$. The carets on the dimensional stability derivatives indicate a type of derivative generally used in roll-coupling analyses. For example,

$$\hat{n}_\beta=\frac{\bar{q}Sb}{I_Y-I_X}C_{n_\beta},\quad y_\beta=\frac{\bar{q}S}{mV}C_{y_\beta}$$

References

[1]Phillips, W.H., "Effect of Steady Rolling on Longitudinal Stability," NASA TN 1627, 1948.

[2]Pinsker, W.J.G., "Aileron Control of Small Aspect Ratio Aircraft in Particular, Delta Aircraft," Ames Research Center, R and M 3188, 1953.

[3]Rhoads, D.W. and Schuler, J.M., "A Theoretical and Experimental Study of Airplane Dynamics in Large-Disturbance Maneuvers," *Journal of Astronautical Sciences*, Vol. 24, July 1957, pp. 507-526, 532.

[4]Hacker, T. and Oprisiu, C., "A Discussion of the Roll Coupling Problem," *Progress in Aerospace Sciences*, Vol. 15, Pergamon Press, Oxford, 1974.

[5]Schy, A.A. and Hannah, M.E., "Prediction of Jump Phenomena in Roll Coupled Maneuvers of Airplanes," *Journal of Aircraft*, Vol. 14, April 1977, pp. 375-382.

[6]Adams, W.M., Jr., "Analytic Prediction of Aircraft Equilibrium Spin Characteristics," NASA TN D-6926, 1972.